

Hydrogen Sulfide Diminishes Activation of Adventitial Fibroblasts Through the Inhibition of Mitochondrial Fission

Zhao-Yang Lu, PhD, MD,*† Chun-Ling Guo, MD,* Bin Yang, PhD, MD,* Yao Yao, MD,* Zhuo-Jing Yang, MD,*† Yu-Xin Gong, MD,*† Jing-Yao Yang, MD,*† Wen-Yuan Dong, MD,* Jun Yang, MD,* Hai-Bing Yang, MD,‡ Hui-Min Liu, PhD, MD,†§ and Bao Li, PhD, MD*

Abstract: Activation of adventitial fibroblasts (AFs) on vascular injury contributes to vascular remodeling. Hydrogen sulfide (H₂S), a gaseous signal molecule, modulates various cardiovascular functions. The aim of this study was to explore whether exogenous H₂S ameliorates transforming growth factor- β 1 (TGF- β 1)-induced activation of AFs and, if so, to determine the underlying molecular mechanisms. Immunofluorescent staining and western blot were used to determine the expression of collagen I and α -smooth muscle actin. The proliferation and migration of AFs were performed by using cell counting Kit-8 and transwell assay, respectively. The mitochondrial morphology was assessed by using MitoTracker Red staining. The activation of signaling pathway was evaluated by western blot. The mitochondrial reactive oxygen species and mitochondrial membrane potential were determined by MitoSOX

and JC-1 (5,5',6,6'-tetrachloro-1,1,3,3'-tetraethylbenzimidazolyl carbocyanine iodide) staining. Our study demonstrated exogenous H₂S treatment dramatically suppressed TGF- β 1-induced AF proliferation, migration, and phenotypic transition by blockage of dynamin-related protein 1 (Drp1)-mediated mitochondrial fission and regulated mitochondrial reactive oxygen species generation. Moreover, exogenous H₂S reversed TGF- β 1-induced mitochondrial fission and AF activation by modulating Rho-associated protein kinase 1-dependent phosphorylation of Drp1. In conclusion, our results suggested that exogenous H₂S attenuates TGF- β 1-induced AF activation through suppression of Drp1-mediated mitochondrial fission in a Rho-associated protein kinase 1-dependent fashion.

Key Words: Hydrogen sulfide, adventitial fibroblasts, dynamin-related protein 1, mitochondrial fission

(*J Cardiovasc Pharmacol*TM 2022;79:925–934)

Received for publication September 9, 2021; accepted February 9, 2022.

From the *Department of Cardiology, The Second Hospital of Shanxi Medical University, Taiyuan, China; †Key Laboratory of Cellular Physiology at Shanxi Medical University, Ministry of Education, and the Department of Physiology, Shanxi Medical University, Taiyuan, China; ‡Department of Cardiology, Yingshang First Hospital, Fuyang, China; and §Department of Hematology, The Second Hospital of Shanxi Medical University, Taiyuan, China.

Supported by the China National Natural Science Foundation (81800171, 81900275), the Natural Science Foundation of Shanxi Province (201801D221273), the Scientific and Technological Innovation Program of Shanxi Higher Education Institution (201804026, 201804027), and Shanxi Provincial Commission of Health and Family Planning (2017053).

The authors report no conflicts of interest.

Z.-Y. Lu performed the experiments, designed study, and analyzed data; C.-L. Guo and B. Yang performed the experiments and analyzed data; Y. Yao performed the experiments; Z.-J. Yang cultured cell; Y.-X. Gong, J.-Y. Yang, W.-Y. Dong, and J. Yang performed the experiments; H.-B. Yang analyzed data; H.-M. Liu designed study and wrote the manuscript; B. Li designed entire research.

Z.-Y. Lu, and C.-L. Guo contributed equally to this work.

Correspondence: Bao Li, PhD, MD, Department of Cardiology, The Second Hospital of Shanxi Medical University, 382 Wuyi Rd, Taiyuan, Shanxi 030001, China (e-mail: libaoxys@163.com) or Hui-Min Liu, PhD, MD, Department of Hematology, The Second Hospital of Shanxi Medical University, 382 Wuyi Rd, Taiyuan, Shanxi 030001, China (e-mail: flysharon@126.com) or Hai-Bing Yang, MD, Department of Cardiology, Yingshang First Hospital, Yingli Rd, Fuyang 236000, China (e-mail: yanghb20@163.com).

Copyright © 2022 The Author(s). Published by Wolters Kluwer Health, Inc. This is an open access article distributed under the terms of the Creative Commons Attribution-Non Commercial-No Derivatives License 4.0 (CCBY-NC-ND), where it is permissible to download and share the work provided it is properly cited. The work cannot be changed in any way or used commercially without permission from the journal.

INTRODUCTION

Cardiovascular disease is a worldwide problem and the leading cause of death.¹ Vascular remodeling is a common trait of several cardiovascular diseases, including atherosclerosis and restenosis after angioplasty.² The vessel consists of 3 distinct layers: intima, media, and adventitia. The adventitia has long been regarded as an “inert” layer providing support and nourishment for the blood vessel. Contrary to this notion, growing evidence indicate that the adventitia is a critical regulator of vessel wall structure and function.³ Recently, the contribution of adventitial fibroblasts (AFs) to vascular remodeling has gained growing attention.⁴ In response to vascular injury, such as after angioplasty, AFs are activated and undergo a phenotypic switch to myofibroblasts (MFs),^{3,5} which are characterized by higher proliferative and migratory activities, upregulated expression of α -smooth muscle actin (α -SMA), and extracellular matrix proteins. It is well-established that transforming growth factor- β 1 (TGF- β 1) plays a prominent role in vascular remodeling processes after angioplasty by inducing activation of AFs.⁶ Thus, further research on TGF- β 1-induced vascular remodeling may conduce to identification of new pathways to prevent vascular remodeling.

Mitochondria are subcellular organelles that play critical roles in regulating many physiological and pathophysiological processes of cellular.^{7,8} A recent study demonstrated that mitochondrial dynamics, particularly mitochondrial fission and fusion, are closely associated with mitochondrial homeostasis.⁹ In mammals, the processes of mitochondrial fission and fusion

are mainly mediated by dynamin-related protein 1 (Drp1) and mitofusins (1/2), respectively. Disruptions in the fusion/fission balance have been implicated in various human diseases, including cardiovascular diseases.¹⁰ Particularly, multiple lines of evidence, including from our investigation, manifests that Drp1-dependent mitochondrial fission is associated with hypertension-induced phenotypic transformation of vascular smooth muscle cells (VSMCs) and hyperglycemia-induced endothelial apoptosis.^{11–13} However, little is known regarding whether mitochondrial fission regulates the phenotypic transition of AFs induced by TGF- β 1.

Hydrogen sulfide (H₂S) has long been considered a malodorous and toxic gas¹⁴; but recently, H₂S has been identified as the third gaseous messenger, along with nitric oxide and carbon monoxide, and it plays a pivotal role in a wide variety of physiology and pathophysiology processes.^{15,16} Emerging studies indicate that H₂S possesses a variety of cardiovascular protective effects because of its antioxidant, anti-inflammatory, and antiapoptotic effects.^{17,18} H₂S can attenuate coronary artery wall thickness in the spontaneously hypertensive rats by downregulating reactive oxygen species (ROS).¹⁹ H₂S can prevent myocardial hypertrophy in the rat model of abdominal aortic constriction by upregulating connexin 43.²⁰ H₂S can also reduce smoking-induced increase of left ventricular mass.²¹ Indeed, our latest study indicated that H₂S from diallyl trisulfide attenuates hyperglycemia-induced endothelial apoptosis and hypertension-induced phenotypic switch of VSMCs by decreasing mitochondrial fission.^{12,13} Furthermore, recent data suggested that H₂S from diallyl disulfide inhibits cancer cell proliferation and migration through inhibition of Rho-associated protein kinase 1 (ROCK1),^{22,23} and ROCK1 activation regulates mitochondrial fission in podocytes and endothelial cells.²⁴ However, to the best of our knowledge, it is still not clear whether exogenous H₂S can attenuate the activation of AFs induced by TGF- β 1.

The major goal of this study was therefore to determine whether exogenous H₂S can ameliorate AF activation induced by TGF- β 1 and, if so, to clarify the mechanism(s) of this effect.

METHODS

AF Cell Culture and Treatment

Primary AFs were isolated from normal thoracic aortas of 16-week-old male C57BL/6J mice have been previously described.²⁵ AFs were cultured with Dulbecco's modified Eagle medium (DMEM) containing 10% fetal bovine serum, 100 U/mL penicillin, and 0.1 mg/mL streptomycin in a humidified incubator with 5% CO₂ at 37°C. AFs were used from passages 3 to 6 in the experiments. Before each experiment, AFs were made quiescent by incubation in serum-free DMEM for 24 hours. AFs were treated with TGF- β 1 (10 ng/mL), with or without sodium hydrosulfide (NaHS, an exogenous H₂S donor, 100 μ mol/L), for 24 hours.

Cell Immunofluorescent Staining

AFs were fixed with 4% paraformaldehyde for 20 minutes at room temperature, permeabilized with 0.2% Triton X-100 for 20 minutes, and then incubated with 5% bovine

serum albumin for 30 minutes at room temperature. Next, AFs were incubated with primary antibody against α -SMA (1:100, Cat No. 19245; Cell Signaling Technology) at 4°C overnight in a humid chamber, followed by incubation with fluorescence-conjugated secondary antibody (1:400, Cat No. 111-585-003; Jackson ImmunoResearch) for 1 hour at room temperature. Finally, cell nuclei were labeled with 4',6-diamidino-2-phenylindole. The images were obtained using a fluorescence microscope.

Cell Proliferation Assay

A cell counting Kit-8 (Dojindo, Japan) was used to detect cell proliferation. In brief, AFs were seeded into 96-well plates at 5×10^3 cells/well. AFs were starved in serum-free DMEM for 24 hours. Then, cells were treated with various treatments according to different experiment groups. Cells were cultured for 2 hours at 37°C after adding cell counting Kit-8 solution (10 μ L/well). The absorbance value was analyzed at 450 nm in a microplate reader.

For cell counting, AFs were added into 6-well plates at 1×10^5 cells/well. AFs were starved in serum-free DMEM for 24 hours. After the above-mentioned treatments, cells were trypsinized and counted on a hemocytometer while capturing them using an inverted microscope.

Transwell Assay

Cell migration was determined by a 24-well plate transwell chamber with 8- μ m pore size and a polycarbonate membrane (Corning, Cambridge, MA). Cultured AFs were synchronized with serum starvation, and cells were seeded into the upper chamber at a density of 2×10^4 cells/well. Then, NaHS or TGF- β 1 was added to the lower compartment of the chamber for 24 hours. AFs adhering beneath the membrane were fixed with ice cold methanol and stained with crystal violet (Beyotime, Haimen, China). The cells that migrated into the lower chamber were quantified by a light microscopy.

Western Blotting

Total proteins were extracted from cultured AFs, and western blotting was performed as briefly mentioned below. Protein concentrations were quantified by bicinchoninic acid protein assay kit (Pierce, Rockford, IL). An equal amount of protein from each lysate (20 μ g) was separated by 10% sodium dodecyl sulfate–polyacrylamide gel electrophoresis, followed by transferring onto nitrocellulose membranes. Membranes were blocked with 5% milk for 1 hour at room temperature, and the membrane was incubated with primary antibodies against Drp1 (1:1000, sc-271583; Santa Cruz Biotechnology), pDrp1 (1:1000, Cat No. 3455; Cell Signaling Technology), ROCK1 (1:1000, Cat No. 4035; Cell Signaling Technology), collagen I (1:1000, Cat No. 72,026; Cell Signaling Technology), α -SMA (1:1000, Cat No. 19,245; Cell Signaling Technology), and glyceraldehyde-3-phosphate dehydrogenase (1:1000, Cat #No. 5174; Cell Signaling Technology) overnight at 4°C. After incubation with secondary antibodies (1:3000, Cat No. 111-035-003, Cat No. 115-035-003; Jackson ImmunoResearch) for 1 hour at room temperature, membranes were detected by using

the enhanced chemiluminescence western blotting detection system (Amersham Pharmacia, Deisenhofen, Germany).

siRNA Transfection

Specific small interfering RNA (siRNA) targeting ROCK1 and Drp1 was purchased from Santa Cruz Biotechnology. Transfection of siRNA was performed using Lipofectamine 2000 Reagent (Invitrogen, Carlsbad, CA) according to the manufacturer's protocol.

Mitochondrial Morphology

To quantify mitochondrial morphology, AFs were seeded onto coverslips. After the treatments, cells were stained with MitoTracker Red (25 nM, Molecular Probes) for 20 minutes at 37°C. Then, we captured mitochondria with a confocal microscope (Zeiss LSM510 META). The mitochondrial morphologies were divided into 3 classifications: tubular (>4 μm in length), intermediate (2–4 μm in length), and fragmented (<2 μm in length). Morphometric analyses of mitochondria were performed by using Image J software as described previously.¹²

Assessment of mtROS and Membrane Potential

To determine mitochondrial ROS (mtROS), AFs were incubated with 5 μM MitoSOX (Invitrogen) for 10 minutes before fixation with 4% paraformaldehyde. The fluorescent images were captured with an Olympus fluorescent microscope. The fluorescence intensity was quantified by Image J software (National Institutes of Health, Bethesda, MD). To evaluate mitochondrial membrane potential, AFs were stained with 200 nM JC-1 (5,5',6,6'-tetrachloro-1,1,3,3'-tetraethylbenzimidazolyl carbocyanine iodide; Beyotime) for 30 minutes. Fluorescent images were obtained by using an Olympus fluorescent microscope. The ratio of red/green fluorescence was used to determine mitochondrial membrane potential.

Statistical Analysis

The results were presented as mean ± standard error of the mean values. Student's *t* test (2-tailed, unpaired) was used for comparison of 2 groups, and the 2-way analysis of the variance test was used for comparison of multiple groups, followed by Tukey's post hoc test. A value of *P* < 0.05 was considered significant.

RESULTS

Exogenous H₂S Ameliorated TGF-β1-Induced AF Phenotype Switching, Proliferation, and Migration

To calculate the effective doses of exogenous H₂S on AF proliferation, a dose-response study with varying doses (10, 50, 100, and 200 μmol/L) of NaHS for 24 hours was performed. As shown in Figure 1A, NaHS did not alter AF cell viability, whereas the doses of NaHS from 10 to 200 μmol/L markedly inhibited TGF-β1-induced AF cell proliferation, with a maximal effect at 100 μmol/L (Fig. 1B).

To compare the precise effect of NaHS, further experiments were performed using NaHS at the concentration of 100 μmol/L.

We first assessed the effects of exogenous H₂S on TGF-β1-induced AF phenotype conversion. Immunofluorescence staining and western blotting indicated that treating AFs with TGF-β1 can cause them to differentiate into a MF phenotype, which was marked by α-SMA and collagen I upregulation (Figs. 1C–F). However, exogenous H₂S dramatically inhibited the TGF-β1-induced phenotypic transition of AFs. Next, we tested the effects of exogenous H₂S on TGF-β1-induced AF proliferation by cell proliferation assay. The results revealed that exogenous H₂S significantly inhibited TGF-β1-induced cell proliferation (Figs. 1G, H). Furthermore, the transwell experiment was used to determine the migration of cells; the results revealed that the TGF-β1-induced cell migration was inhibited by exogenous H₂S (Figs. 1I, J).

Drp1-Mediated Mitochondrial Fission is Required for TGF-β1-Induced AF Activation

A recent study has showed that Drp1-mediated mitochondrial fission involves in AF proliferation and migration, which shows that mitochondrial fission may be required for cell phenotype shift.²⁵ In this study, we examined the role of Drp1-mediated mitochondrial fission in TGF-β1-induced AF activation. As exhibited in Figures 2A, B, Drp1 siRNA successfully prevented Drp1 expression. In addition, MitoTracker Red staining and confocal microscopy studies showed that TGF-β1 stimulation substantially increased mitochondrial fission in AF. However, Drp1 inhibition by gene silencing completely prevented this effect (Figs. 2C, D).

To further determine the role of mitochondrial fission on the biological functions of TGF-β1-induced AFs, we next observed the effect of Drp1 inhibition on TGF-β1-induced phenotype switching, proliferation, and migration. Western blot assay showed that the downregulation of Drp1 by siRNA ameliorated TGF-β1-induced AF phenotypic switch to MF (Figs. 2E–G). Cell proliferation assays revealed that Drp1 siRNA prevented TGF-β1-induced AF proliferation (Figs. 2H, I). In addition, transwell migration assay manifested that Drp1 siRNA attenuated TGF-β1-induced AF migration (Figs. 2J, K).

ROCK1 Is Involved in Mediating TGF-β1-Induced Mitochondrial Fission

ROCK1 has been reported to phosphorylate Ser616 in Drp1 in various types of cells.^{12,26} In addition, ROCK1 is involved in numerous pathological and physiological processes of cardiovascular diseases. This prompted us to determine whether Drp1 phosphorylation at serine 616 is involved in the process of TGF-β1-induced mitochondrial fission. As presented in Figures 3A, B, ROCK1 siRNA successfully suppressed ROCK1 expression. MitoTracker Red staining indicated that ROCK1 inhibition by siRNA significantly decreased the effects of TGF-β1 on mitochondrial fission (Figs. 3C, D). Furthermore, ROCK1 inhibition ameliorated

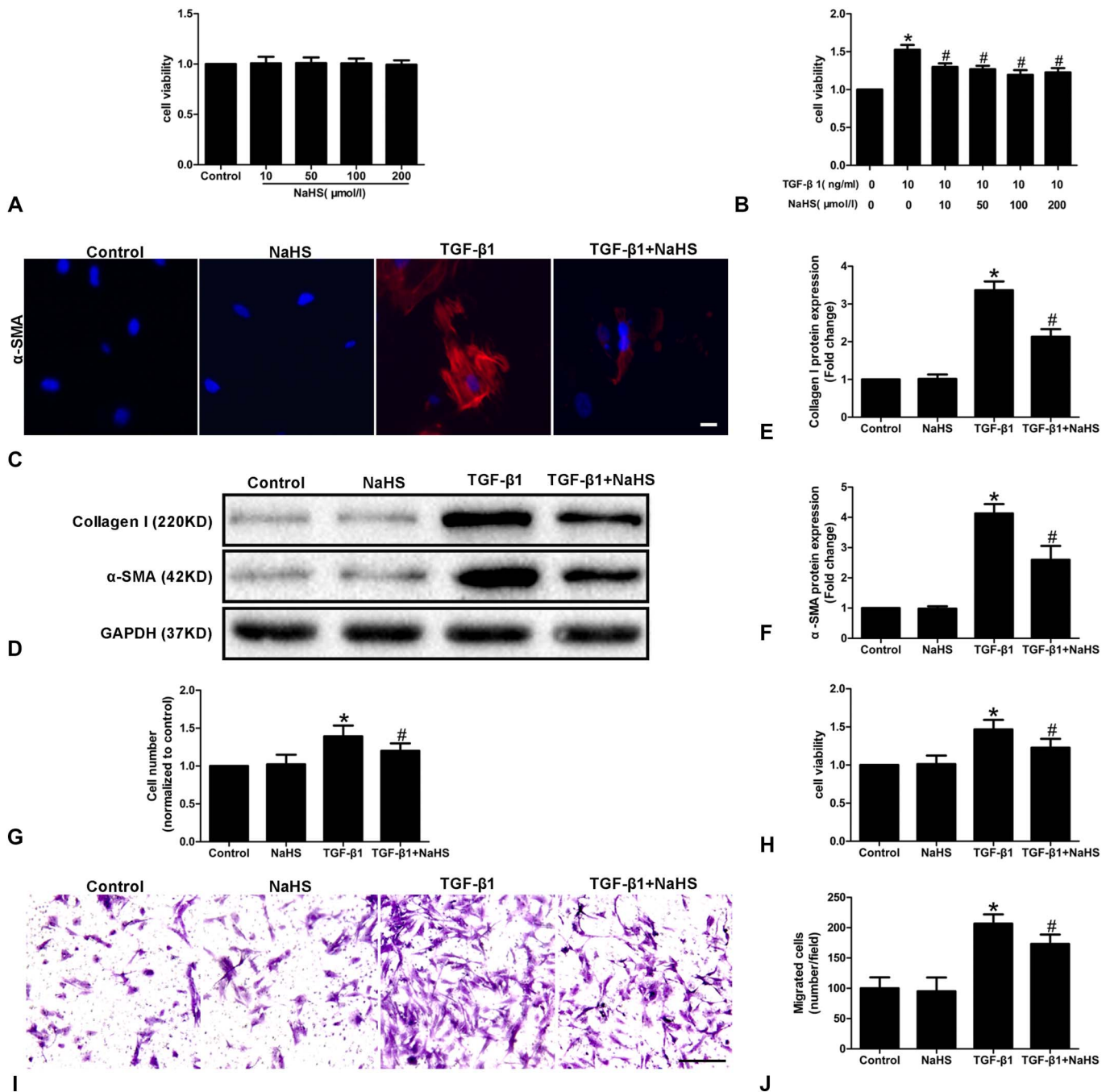


FIGURE 1. Exogenous H₂S ameliorated TGF-β1–induced AF phenotype switching, proliferation, and migration. AFs were pre-treated with or without NaHS (100 μM) or vehicle for 1 hour, then were stimulated with TGF-β1 (10 ng/mL) for 24 hours. A, B, Quantification by cell counting Kit-8 assay. C, AF phenotype switching indicated by the expression of α-SMA was determined by immunofluorescence staining. Scale bar = 20 μm. D, The expression of collagen I and α-SMA was determined by western blotting. E, Quantitative analysis for collagen I. F, Quantitative analysis for α-SMA. G, H, Quantification by cell counting and cell counting Kit-8 assay. I, Representative images of transwell migration assay. Scale bar = 100 μm. J, Quantification of migrated cells. Values are represented as means ± standard error of the mean (n = 3); *P < 0.05 versus control group; #P < 0.05 versus TGF-β1 group.

TGF-β1–induced Drp1 (Ser616) phosphorylation in AFs (Figs. 3E, F).

To further determine the effect of ROCK1 on AF activation under TGF-β1 treatment, the phenotype switching,

proliferation, and migration of AF were further performed. As shown in Figs. 3G–M, ROCK1 inhibition dramatically suppressed TGF-β1–induced AF phenotypic, proliferation, and migration. These results showed that ROCK1 mediated TGF-

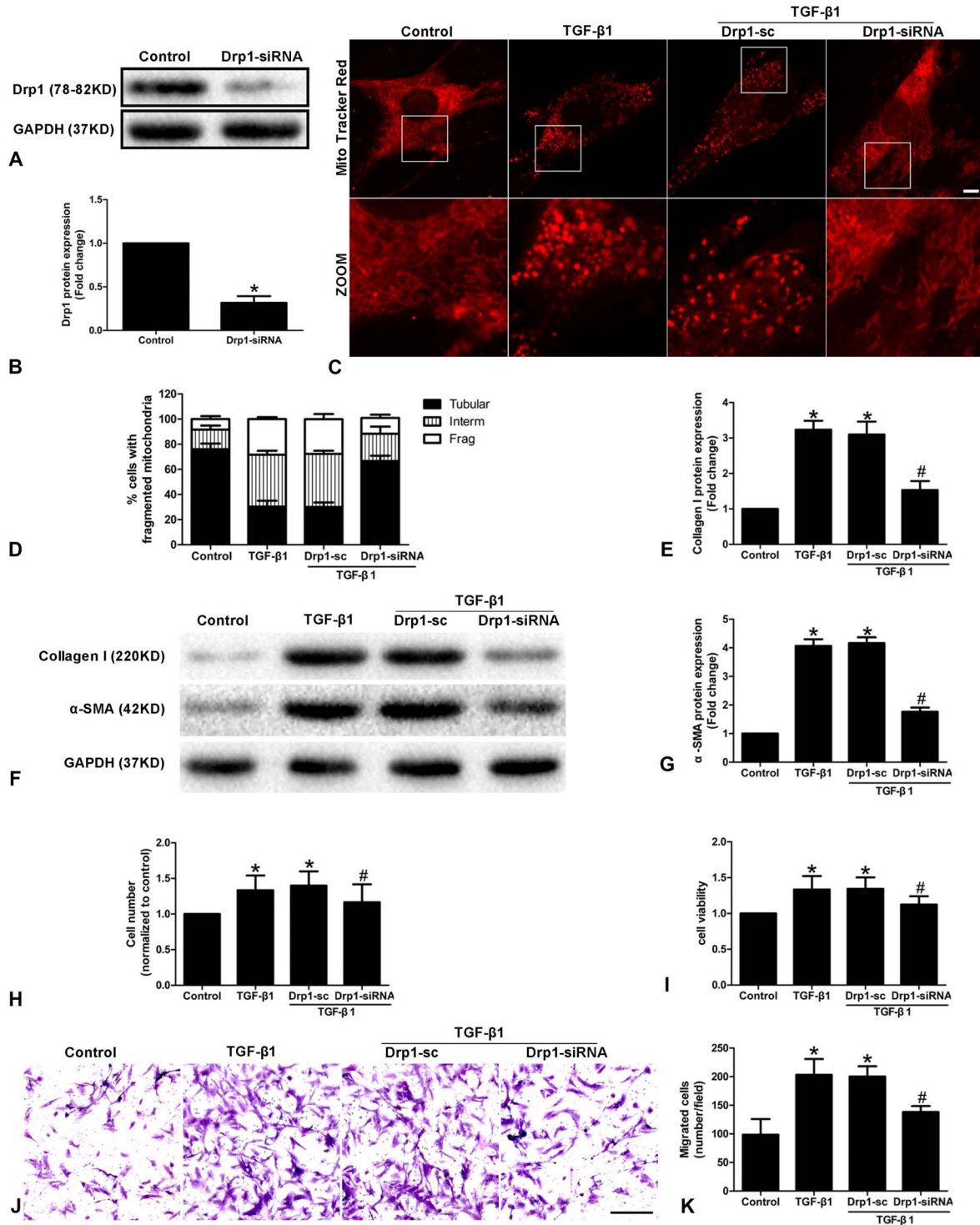


FIGURE 2. Drp1-mediated mitochondrial fission is required for TGF-β1-induced AF activation. AFs were transfected with Drp1 siRNA or scrambled siRNA, followed by treatment with TGF-β1 (10 ng/mL) for 24 hours. A, B, The expression of Drp1 was determined by western blotting. C, Micrographs of mitochondrial morphology stained by MitoTracker Red of AFs. Scale bar = 10 μm. D, Quantification of mitochondrial morphology. E, Quantitative analysis for collagen I. F, The expression of collagen I and α-SMA was determined by western blotting. G, Quantitative analysis for α-SMA. H, I, Quantification by cell counting Kit-8 assay and cell counting. J, Representative images of transwell migration assay. Scale bar = 100 μm. K, Quantification of migrated cells. Values are represented as means ± standard error of the mean (n = 3); *P < 0.05 versus control group; #P < 0.05 versus TGF-β1 group.

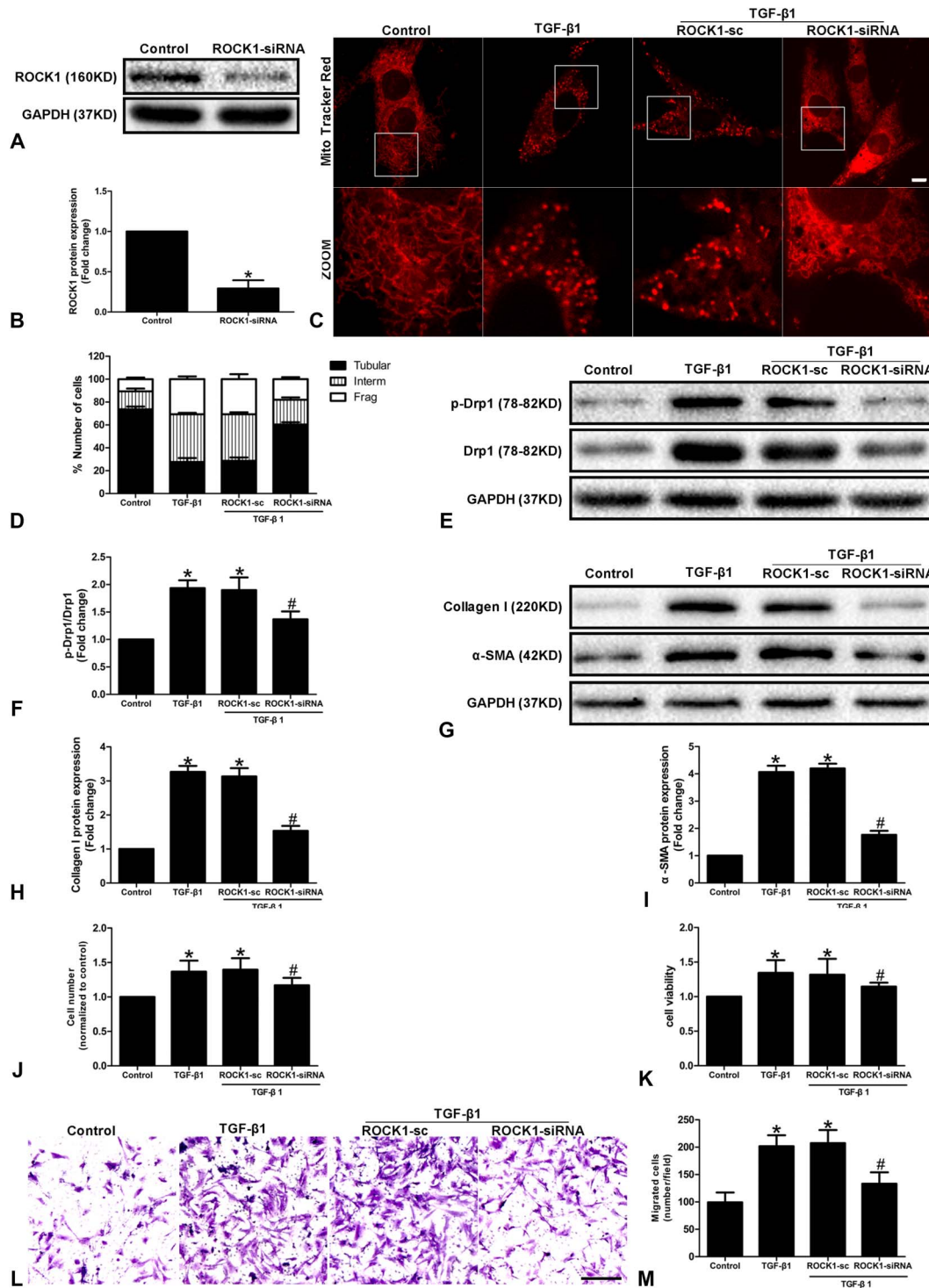


FIGURE 3. ROCK1 is involved in mediating TGF-β1-induced mitochondrial fission. AFs were transfected with ROCK1 siRNA or scrambled siRNA, followed by treatment with TGF-β1 (10 ng/mL) for 24 hours. A, B, The expression of ROCK1 was determined by western blotting. C, Micrographs of mitochondrial morphology stained by MitoTracker Red of AFs. Scale bar =10 μm. D, Quantification of mitochondrial morphology. E, The expression of pDrp1 and Drp1 were determined by western blotting. F, Quantitative analysis for pDrp1. G, The expression of collagen I and α-SMA was determined by western blotting. H, Quantitative analysis for collagen I. I, Quantitative analysis for α-SMA. J, K, Quantification by cell counting Kit-8 assay and cell counting. L, Representative images of transwell migration assay. Scale bar =100 μm. M, Quantification of migrated cells. Values are represented as means ± standard error of the mean (n = 3); *P < 0.05 versus control group; #P < 0.05 versus TGF-β1 group.

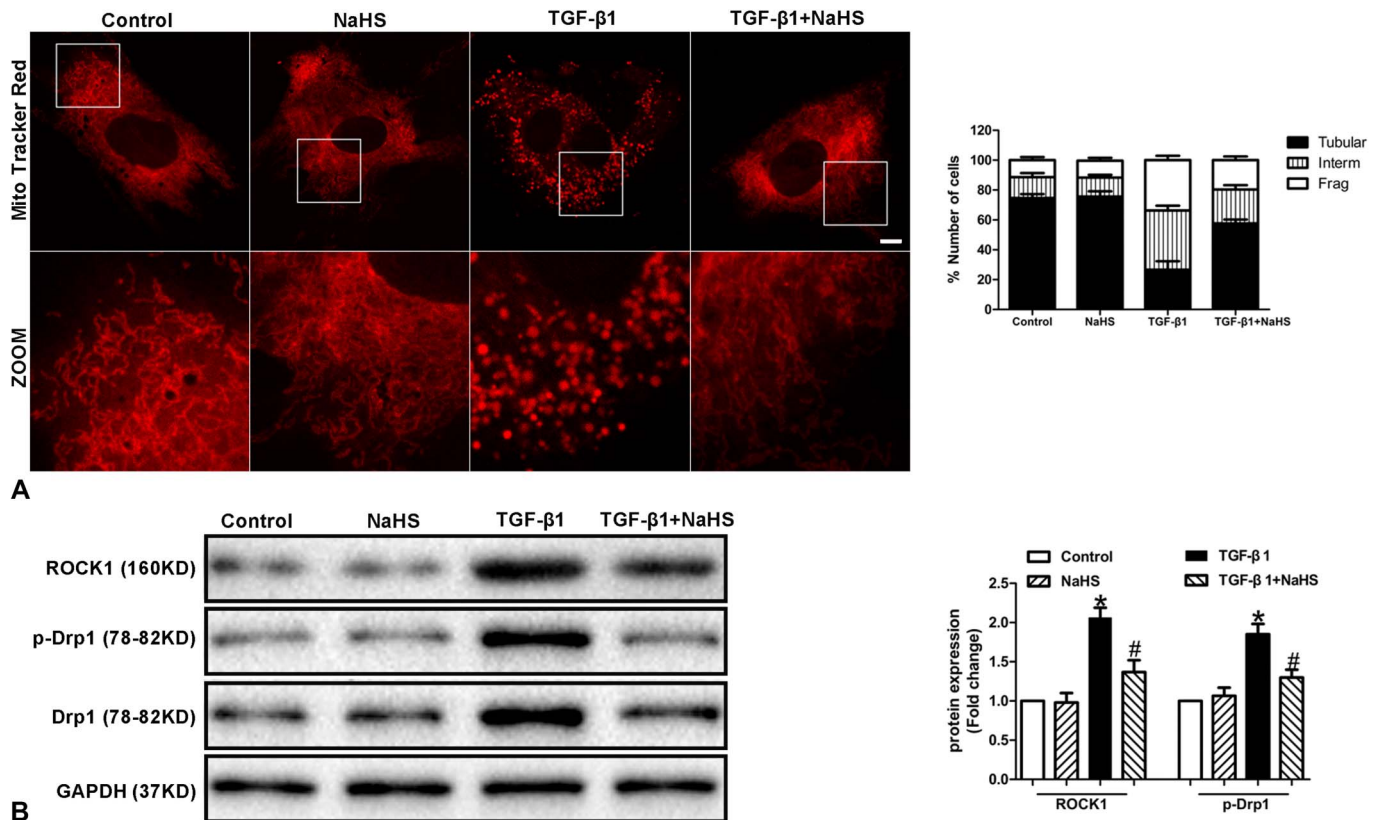


FIGURE 4. Exogenous H₂S inhibited TGF-β1–induced mitochondrial fission. AFs were pretreated with or without NaHS (100 μM) for 1 hour, then were stimulated with TGF-β1 (10 ng/mL) or vehicle for 24 hours. **A**, Micrographs of mitochondrial morphology visualized by MitoTracker Red staining of AFs and quantification of mitochondrial morphology. Scale bar =10 μm. **B**, The expression of ROCK1 and pDrp1 were determined by western blotting. Values are represented as means ± standard error of the mean (n = 3); *P < 0.05 versus control group; #P < 0.05 versus TGF-β1 group.

β1–induced mitochondrial fission and subsequent AF activation.

Exogenous H₂S Inhibited TGF-β1–Induced Mitochondrial Fission

Exogenous H₂S reportedly inhibit VSMC activation by modulating mitochondrial fission.²⁷ Herein, we determined the effect of exogenous H₂S on mitochondrial fission in AFs. As shown in Figure 4A, exogenous H₂S significantly reversed the TGF-β1–induced mitochondrial fission in AFs. Next, we evaluated the effects of TGF-β1 and exogenous H₂S on the ROCK1/Drp1 pathway by western blotting assay. We found that TGF-β1 upregulated ROCK1 expression and Drp1 (Ser616) phosphorylation, whereas exogenous H₂S successfully prevented the TGF-β1–induced ROCK1/Drp1 pathway activation (Fig. 4B).

Exogenous H₂S Ameliorated mtROS in TGF-β1–Induced AF

Previous studies have reported that DRP1-regulated mitochondrial fission is an upstream regulator of mtROS generation, leading to mitochondrial dysfunction.^{18,28,29} TGF-β1 has been reported to increase Drp1-mediated mitochondrial fission and subsequent generation of mtROS,³⁰

and mtROS have also been found to get involved in the processes of cell phenotype switching, proliferation, and migration.^{25,31} We determined whether the TGF-β1 stimulation affects the generation of mtROS in AFs by MitoSOX staining. We observed mtROS significantly increased on TGF-β1 treatment, whereas exogenous H₂S alleviated the TGF-β1–induced mtROS increase (Fig. 5A). As the changes of mitochondrial membrane potential may affect the distribution of MitoSOX,³² we then tested changes of mitochondrial membrane potential by JC-1 staining. We found that TGF-β1 treatment significantly reduced the mitochondrial membrane potential in JC-1–stained AFs. By contrast, exogenous H₂S was able to robustly restore the TGF-β1–induced reduction of mitochondrial membrane potential (Fig. 5B).

To verify the role of ROS, we tested the effect of Mito-TEMPO (a specific scavenger of mitochondrial superoxide) and exogenous ROS on the AF phenotypic transition. Treatment with Mito-TEMPO dramatically decreased the TGF-β1–induced AF response, and the inhibition effect was enhanced by NaHS exposure (Fig. 5C). By contrast, H₂O₂ treatment was able to mimic the TGF-β1–induced effect, and this effect was partially reversed with NaHS treatment (Fig. 5D). These results manifested that the generation of

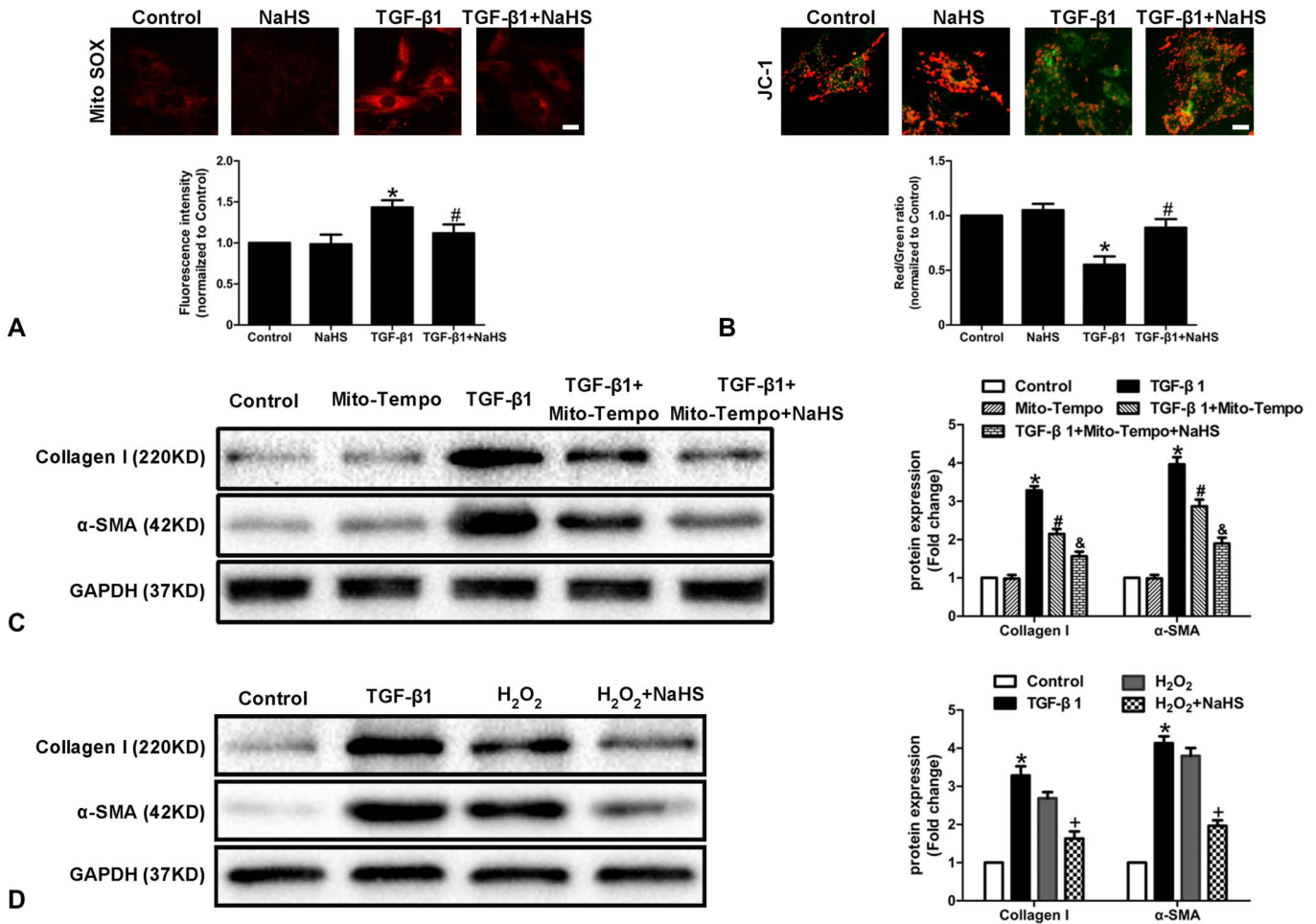


FIGURE 5. Exogenous H₂S ameliorated mtROS in TGF-β1-induced AF. AFs were pretreated with or without NaHS (100 μM) for 1 hour, then were stimulated with TGF-β1 (10 ng/mL) or vehicle for 24 hours. A, Representative graphs and quantification of mitochondrial superoxide determined by MitoSOX. Scale bar = 20 μm. B, Representative images and quantification of mitochondrial membrane potential evaluated by the red/green ratio of JC-1. Scale bar = 20 μm. The effect of Mito-TEMPO (C) and H₂O₂ (D) treatment for 1 hour on AF phenotypic shift indicated by the expression of collagen I and α-SMA were assessed by western blotting. Values are represented as means ± standard error of the mean (n = 3); *P < 0.05 versus control group; #P < 0.05 versus TGF-β1 group; &P < 0.05 versus TGF-β1+Mito-TEMPO group; +P < 0.05 versus H₂O₂ group.

mtROS might be in part account for the effects of TGF-β1 and exogenous H₂S on AF phenotypic switch.

DISCUSSION

In this investigation, we reveal a novel mechanism by which exogenous H₂S ameliorates phenotypic conversion of AFs to MFs induced by TGF-β1. We found that ROCK1/Drp1-dependent mitochondrial fission mediates TGF-β1-induced AF activation, while exogenous H₂S mitigates ROCK1 expression and subsequent Drp1 activation, elucidating a protective role of exogenous H₂S in pathological vascular remodeling by modulating the responses of AFs. Indeed, NaHS showed an obvious protective effect on TGF-β1-induced AFs rather than control AFs, which may be due to the more evident positive effect of NaHS on vascular injury responses rather than reserved.

Our data indicated that exogenous H₂S might be a novel therapeutic strategy for preventing the development of pathological vascular remodeling.

Accumulating evidence indicates that vascular remodeling was an “adventitia-based” process. As the primary cell type of adventitia, AFs have been reported to be the earliest activated cells during vascular remodeling.³³ After vascular injury, AFs are immediately activated and transformed into MFs, in which TGF-β1 acts as a critical modulator. Moreover, exogenous H₂S plays a pivotal role in a wide range of physiological and pathological processes in the cardiovascular system. Emerging data indicate that H₂S improves diabetic endothelial dysfunction,³⁴ inhibits myocardial apoptosis after myocardial infarction,³⁵ and inhibits VSMC proliferation and migration induced by hyperglycaemia²⁷; recent data from our laboratory and others revealed that exogenous H₂S attenuates angiotensin II (Ang II)-induced VSMC phenotypic

switch and vascular remodeling.^{12,36} However, there are no published literature on the potential effect of exogenous H₂S on AF activation. Our study found that TGF-β1 induced AF phenotype switching, proliferation, and migration, which were ameliorated by exogenous H₂S administration.

Mitochondria exist in dynamic networks between fragmented and fused states, and mitochondrial dynamics is regulated by fission and fusion.^{8,26} Abnormal mitochondrial fission is involved in the regulation of mitochondrial fragmentation and damage cellular physiological function and activity.³⁷ Recent investigations show that excessive mitochondrial fission leads to increased apoptosis in endothelial cells induced by hyperglycemia.^{13,38} Moreover, our previous studies indicate that abnormal mitochondrial fission mediates VSMC activation and AF activation induced by Ang II.^{12,25} In this study, we determined whether mitochondrial fission participated in TGF-β1-induced AF activation. We found that TGF-β1 was able to induce mitochondrial fission, and Drp1-mediated mitochondrial fission lead to AF activation.

Drp1, a member of the dynamin family of GTPases, is an important mediator of mitochondrial division. When activated, Drp1 triggers mitochondrial fission. A recent study shows that Ang II-induced Drp1 activation and Drp1-dependent mitochondrial fission participate in AF activation and adventitial remodeling.²⁵ Our current investigation also showed that TGF-β1 significantly increased Drp1 phosphorylation in AFs along with increased fragmented mitochondria. In addition, we revealed that Drp1 siRNA attenuated TGF-β1-induced proliferation, migration, and phenotypic transformation of AFs; these findings are coherent with previous results in other cell types.^{30,39} Our data indicate that Drp1 regulates TGF-β1-induced AF activation. Of note, multiple lines of evidence have suggested Drp1-independent mechanism might also participate in mitochondrial fission process.^{40,41} However, their mechanistic roles in mitochondrial fission remain unknown.

ROCK, a member of serine/threonine family, has been reported to participate in diverse cellular responses, including regulation of cell morphology, proliferation, migration, and differentiation.^{42,43} The ROCK family includes 2 isoforms: ROCK1 and ROCK2. A recent literature has reported that ROCK1 play a critical role in regulating mitochondrial fission by recruiting Drp1 to the mitochondria.⁴⁴ A previous literature demonstrated that ROCK1 activation and Drp1 translocation to the mitochondria are involved in the process of hyperglycemia-induced mitochondrial fission, and this ROCK1-dependent mechanism involves phosphorylation of Drp1 at Ser600. Interestingly, in our previous investigation, we demonstrated that ROCK1 regulates Ang II-induced VSMC activation by mediating the phosphorylation of Drp1 at Ser616 and Drp1-dependent mitochondrial fission.¹² However, whether the ROCK1-dependent metabolic pathway participates in TGF-β1-induced mitochondrial fission and AF activation are still elusive. Our study showed that ROCK1 mediates TGF-β1-induced AF activation by upregulating the phosphorylation of Drp1 at Ser616 and Drp1-dependent mitochondrial fission. Moreover, we found that ROCK1 inhibition attenuated TGF-β1-induced proliferation, migration and

phenotypic switch of AFs. Our results indicated that TGF-β1 may cause AF activation by activating the ROCK1/Drp1 pathway and mitochondrial fission. However, another report showed that ROCK1 may indirectly dephosphorylate Drp1 at Ser637 by activating calcineurin to promote mitochondrial fission in Parkinson's disease.⁴⁵ Illuminating the regulation mechanism between Drp1 and ROCK1 on mitochondrial fission is one of the major areas for future studies.

Exogenous H₂S reportedly protects endothelial cells from high glucose by modulating mitochondrial morphology.⁴⁶ Another literature demonstrated that exogenous H₂S ameliorates VSMC proliferation and migration by regulating mitochondrial fission in a hyperglycemic state.²⁷ In this study, we uncovered that exogenous H₂S dramatically abrogated TGF-β1-induced ROCK1/Drp1-dependent mitochondrial fission and AF activation. In addition, consistent with other cells,^{30,47} TGF-β1 was able to accelerate mitochondrial fission and subsequent mtROS generation in AFs, which was obviously inhibited by exogenous H₂S. It has been reported that inhibition of mitochondrial fission augmented mitochondrial inner membrane proton leak, thus inhibiting PDGF-induced mtROS generation in VSMCs.³¹ The augmented mitochondrial inner membrane proton leak might partly account for the increased mtROS in AFs. Furthermore, our present data establish that Mito-TEMPO obviously suppressed TGF-β1-induced AF phenotypic switch. Meanwhile, exogenous ROS successfully mimicked the TGF-β1-induced effect. Thus, our findings indicate that exogenous H₂S might suppress AF phenotypic transition by inhibiting mtROS generation through the abrogation of TGF-β1-induced mitochondrial fission.

In conclusion, the present data demonstrated that ROCK1/Drp1-dependent mitochondrial fission regulates the TGF-β1-induced AF activation. Moreover, exogenous H₂S could ameliorate TGF-β1-induced AF activation by suppressing ROCK1/Drp1-mediated mitochondrial fission and subsequent mtROS generation. On description of the mechanism conferred by H₂S protection, it is possible to provide a novel approach for therapies in the alleviation of vascular remodeling.

REFERENCES

1. Yang L, Xie P, Wu J, et al. Deferoxamine treatment combined with sevoflurane postconditioning attenuates myocardial ischemia-reperfusion injury by restoring HIF-1/BNIP3-mediated mitochondrial autophagy in GK rats. *Front Pharmacol*. 2020;11:6.
2. Mathew OP, Ranganna K, Mathew J, et al. Cellular effects of butyrate on vascular smooth muscle cells are mediated through disparate actions on dual targets, histone deacetylase (HDAC) activity and PI3K/Akt signaling network. *Int J Mol Sci*. 2019;20:2902.
3. Stenmark KR, Yeager ME, El Kasmi KC, et al. The adventitia: essential regulator of vascular wall structure and function. *Annu Rev Physiol*. 2013;75:23–47.
4. Fu C, Liu P, Li P, et al. FSP1 promotes the biofunctions of adventitial fibroblast through the crosstalk among RAGE, JAK2/STAT3 and Wnt3a/beta-catenin signalling pathways. *J Cell Mol Med*. 2019;23:7246–7260.
5. Coen M, Gabbiani G, Bochaton-Piallat ML. Myofibroblast-mediated adventitial remodeling: an underestimated player in arterial pathology. *Arterioscler Thromb Vasc Biol*. 2011;31:2391–2396.
6. Stenmark KR, Nozik-Grayck E, Gerasimovskaya E, et al. The adventitia: essential role in pulmonary vascular remodeling. *Compr Physiol*. 2011;1:141–161.

7. Tezze C, Romanello V, Desbats MA, et al. Age-associated loss of OPA1 in muscle impacts muscle mass, metabolic homeostasis, systemic inflammation, and epithelial senescence. *Cell Metab.* 2017;25:1374–1389.e6.
8. Anderson GR, Wardell SE, Cakir M, et al. Dysregulation of mitochondrial dynamics proteins are a targetable feature of human tumors. *Nat Commun.* 2018;9:1677.
9. Westermann B. Mitochondrial fusion and fission in cell life and death. *Nat Rev Mol Cell Biol.* 2010;11:872–884.
10. Hall AR, Burke N, Dongworth RK, et al. Mitochondrial fusion and fission proteins: novel therapeutic targets for combating cardiovascular disease. *Br J Pharmacol.* 2014;171:1890–1906.
11. Deng Y, Li S, Chen Z, et al. Mdivi-1, a mitochondrial fission inhibitor, reduces angiotensin-II- induced hypertension by mediating VSMC phenotypic switch. *Biomed Pharmacother.* 2021;140:111689.
12. Lu ZY, Qi J, Yang B, et al. Diallyl trisulfide suppresses angiotensin II-induced vascular remodeling via inhibition of mitochondrial fission. *Cardiovasc Drugs Ther.* 2020;34:605–618.
13. Hao Y, Liu HM, Wei X, et al. Diallyl trisulfide attenuates hyperglycemia-induced endothelial apoptosis by inhibition of Drp1-mediated mitochondrial fission. *Acta Diabetol.* 2019;56:1177–1189.
14. Roorda M, Miljkovic JL, van Goor H, et al. Spatiotemporal regulation of hydrogen sulfide signaling in the kidney. *Redox Biol.* 2021;43:101961.
15. He JT, Li H, Yang L, et al. Role of hydrogen sulfide in cognitive deficits: evidences and mechanisms. *Eur J Pharmacol.* 2019;849:146–153.
16. Hu LF, Wong PT, Moore PK, et al. Hydrogen sulfide attenuates lipopolysaccharide-induced inflammation by inhibition of p38 mitogen-activated protein kinase in microglia. *J Neurochem.* 2007;100:1121–1128.
17. Qin M, Long F, Wu W, et al. Hydrogen sulfide protects against DSS-induced colitis by inhibiting NLRP3 inflammasome. *Free Radic Biol Med.* 2019;137:99–109.
18. Xu D, Jin H, Wen J, et al. Hydrogen sulfide protects against endoplasmic reticulum stress and mitochondrial injury in nucleus pulposus cells and ameliorates intervertebral disc degeneration. *Pharmacol Res.* 2017;117:357–369.
19. Shi YX, Chen Y, Zhu YZ, et al. Chronic sodium hydrosulfide treatment decreases medial thickening of intramyocardial coronary arterioles, interstitial fibrosis, and ROS production in spontaneously hypertensive rats. *Am J Physiol Heart Circ Physiol.* 2007;293:H2093–H2100.
20. Huang J, Wang D, Zheng J, et al. Hydrogen sulfide attenuates cardiac hypertrophy and fibrosis induced by abdominal aortic coarctation in rats. *Mol Med Rep.* 2012;5:923–928.
21. Zhou X, Zhao L, Mao J, et al. Antioxidant effects of hydrogen sulfide on left ventricular remodeling in smoking rats are mediated via PI3K/Akt-dependent activation of Nrf2. *Toxicol Sci.* 2015;144:197–203.
22. Ling H, Ji X, Lei Y, et al. Diallyl disulfide induces downregulation and inactivation of cofilin 1 differentiation via the Rac1/ROCK1/LIMK1 pathway in leukemia cells. *Int J Oncol.* 2020;56:772–782.
23. Su B, Su J, Zeng Y, et al. Diallyl disulfide suppresses epithelial-mesenchymal transition, invasion and proliferation by downregulation of LIMK1 in gastric cancer. *Oncotarget.* 2016;7:10498–10512.
24. Wang W, Wang Y, Long J, et al. Mitochondrial fission triggered by hyperglycemia is mediated by ROCK1 activation in podocytes and endothelial cells. *Cell Metab.* 2012;15:186–200.
25. Huang G, Cong Z, Wang X, et al. Targeting HSP90 attenuates angiotensin II-induced adventitial remodelling via suppression of mitochondrial fission. *Cardiovasc Res.* 2020;116:1071–1084.
26. Shi Y, Fan S, Wang D, et al. FOXO1 inhibition potentiates endothelial angiogenic functions in diabetes via suppression of ROCK1/Drp1-mediated mitochondrial fission. *Biochim Biophys Acta Mol Basis Dis.* 2018;1864:2481–2494.
27. Sun A, Wang Y, Liu J, et al. Exogenous H₂S modulates mitochondrial fusion-fission to inhibit vascular smooth muscle cell proliferation in a hyperglycemic state. *Cell Biosci.* 2016;6:36.
28. Fu P, Epshtein Y, Ramchandran R, et al. Essential role for paxillin tyrosine phosphorylation in LPS-induced mitochondrial fission, ROS generation and lung endothelial barrier loss. *Sci Rep.* 2021;11:17546.
29. Wang Q, Zhang M, Torres G, et al. Metformin suppresses diabetes-accelerated atherosclerosis via the inhibition of Drp1-mediated mitochondrial fission. *Diabetes.* 2017;66:193–205.
30. Wang Y, Lu M, Xiong L, et al. Drp1-mediated mitochondrial fission promotes renal fibroblast activation and fibrogenesis. *Cell Death Dis.* 2020;11:29.
31. Wang L, Yu T, Lee H, et al. Decreasing mitochondrial fission diminishes vascular smooth muscle cell migration and ameliorates intimal hyperplasia. *Cardiovasc Res.* 2015;106:272–283.
32. Polster BM, Nicholls DG, Ge SX, et al. Use of potentiometric fluorophores in the measurement of mitochondrial reactive oxygen species. *Methods Enzymol.* 2014;547:225–250.
33. Lin S, Ma S, Lu P, et al. Effect of CTRP3 on activation of adventitial fibroblasts induced by TGF-beta1 from rat aorta in vitro. *Int J Clin Exp Pathol.* 2014;7:2199–2208.
34. Suzuki K, Olah G, Modis K, et al. Hydrogen sulfide replacement therapy protects the vascular endothelium in hyperglycemia by preserving mitochondrial function. *Proc Natl Acad Sci U S A.* 2011;108:13829–13834.
35. Li Y, Liu M, Yi J, et al. Exogenous hydrogen sulfide inhibits apoptosis by regulating endoplasmic reticulum stress-autophagy axis and improves myocardial reconstruction after acute myocardial infarction. *Acta Biochim Biophys Sin (Shanghai).* 2020;52:1325–1336.
36. Lu HY, Hsu HL, Li CH, et al. Hydrogen sulfide attenuates aortic remodeling in aortic dissection associating with moderated inflammation and oxidative stress through a NO-dependent pathway. *Antioxidants (Basel).* 2021;10:682.
37. Kunieda T, Minamino T, Nishi J, et al. Angiotensin II induces premature senescence of vascular smooth muscle cells and accelerates the development of atherosclerosis via a p21-dependent pathway. *Circulation.* 2006;114:953–960.
38. Bhatt MP, Lim YC, Kim YM, et al. C-peptide activates AMPKalpha and prevents ROS-mediated mitochondrial fission and endothelial apoptosis in diabetes. *Diabetes.* 2013;62:3851–3862.
39. Salabei JK, Hill BG. Mitochondrial fission induced by platelet-derived growth factor regulates vascular smooth muscle cell bioenergetics and cell proliferation. *Redox Biol.* 2013;1:542–551.
40. Nakamura K, Nemani VM, Azarbal F, et al. Direct membrane association drives mitochondrial fission by the Parkinson disease-associated protein alpha-synuclein. *J Biol Chem.* 2011;286:20710–20726.
41. Roy M, Itoh K, Iijima M, et al. Parkin suppresses Drp1-independent mitochondrial division. *Biochem Biophys Res Commun.* 2016;475:283–288.
42. Zhang C, Wu JM, Liao M, et al. The ROCK/GGTase pathway are essential to the proliferation and differentiation of neural stem cells mediated by simvastatin. *J Mol Neurosci.* 2016;60:474–485.
43. Tang L, Dai F, Liu Y, et al. RhoA/ROCK signaling regulates smooth muscle phenotypic modulation and vascular remodeling via the JNK pathway and vimentin cytoskeleton. *Pharmacol Res.* 2018;133:201–212.
44. Zhang Q, Hu C, Huang J, et al. ROCK1 induces dopaminergic nerve cell apoptosis via the activation of Drp1-mediated aberrant mitochondrial fission in Parkinson's disease. *Exp Mol Med.* 2019;51:1–13.
45. Buhlman L, Damiano M, Bertolin G, et al. Functional interplay between Parkin and Drp1 in mitochondrial fission and clearance. *Biochim Biophys Acta.* 2014;1843:2012–2026.
46. Liu N, Wu J, Zhang L, et al. Hydrogen Sulphide modulating mitochondrial morphology to promote mitophagy in endothelial cells under high-glucose and high-palmitate. *J Cell Mol Med.* 2017;21:3190–3203.
47. Wu J, Niu J, Li X, et al. TGF-beta1 induces senescence of bone marrow mesenchymal stem cells via increase of mitochondrial ROS production. *BMC Dev Biol.* 2014;14:21.